informatics

MDPI

Article

Learning-Based Data-Driven Heading Control for Unmanned Surface Vehicles: A Nussbaum-RBF Sliding Mode Approach

Jianlin Zhou, Yuhao Dai, Wentao Xue and Wei Liu *

College of Automation, Jiangsu University of Science and Technology, Zhenjiang 212000, China; 241110303105@stu.just.edu.cn (J.Z.); 241210301208@stu.just.edu.cn (Y.D.); xuewent@just.edu.cn (W.X.)
* Correspondence: liuwei1988@just.edu.cn

Abstract

Owing to unknown hydrodynamic characteristics, unmeasurable external disturbances and uncertain control coefficients, conventional control strategies that rely on precise mechanistic models often suffer from notable performance degradation. To address this problem, a novel data-driven Nussbaum-RBF Sliding Mode Control (NRSMC) strategy is proposed for USV heading control. In the proposed framework, a Radial Basis Function (RBF) neural network is employed as a data-driven approximator to learn unknown nonlinear system dynamics online, avoiding the dependence on accurate prior mathematical models. Based on the online-learned dynamic information, a sliding mode control (SMC) mechanism is developed to enhance robustness against approximation errors and external disturbances, and a boundary layer technique is introduced to alleviate the chattering phenomenon. Furthermore, a Nussbaum function is incorporated to address the unknown control coefficients problem, ensuring system stability without requiring prior knowledge of the control coefficients. The stability of the closed-loop system is rigorously analyzed using Lyapunov theory. Comparative simulation results demonstrate that the proposed NRSMC strategy achieves superior tracking accuracy and robustness compared with the Nussbaum-RBF Adaptive Backstepping Control (NRABC) method. Moreover, field experiments conducted further validate the effectiveness and adaptability of the proposed data-driven control approach.

Keywords: USV; data-driven control; RBF neural network; sliding mode control; Nussbaum gain

Check for updates

Academic Editors: Weitian Tong, Lei Chen and Lixin Li

Received: 9 July 2026
Revised: 22 August 2026
Accepted: 3 September 2026
Published: 7 September 2026

Copyright: © 2026 by the authors. Licensee MDPI, Basel, Switzerland. This article is an open access article distributed under the terms and conditions of the Creative Commons Attribution (CC BY) license.

1. Introduction

With the rapid development of marine resource exploration, intelligent maritime systems, and autonomous marine vehicles, unmanned surface vehicles (USVs) have attracted increasing attention due to their advantages of compact structure, high maneuverability, and autonomous operation capabilities. They have been widely applied in various fields, including hydrographic surveying, military reconnaissance, environmental monitoring, and maritime search and rescue [1–3]. As a fundamental component of autonomous navigation, heading control plays a crucial role in ensuring accurate trajectory tracking, motion stability, and operational safety of USVs [4–6].

Traditional control approaches, including backstepping [7], linear quadratic regulator (LQR) [8], and model predictive control (MPC) [9], have been extensively investigated for USVs due to their theoretical effectiveness and clear control structures. However, these

methods generally rely on accurate mathematical models and prior knowledge of hydrodynamic parameters. USVs typically operate in highly dynamic marine environments characterized by nonlinear hydrodynamic effects and uncertain environmental disturbances caused by wind, waves, and ocean currents [10]. Moreover, the nonlinear characteristics of USV dynamics and unknown environmental disturbances make it difficult to identify hydro-dynamic parameters and accurately describe the varying system [11,12]. Therefore, developing an adaptive heading control strategy without relying on accurate mechanistic models and enhanced environmental adaptability remains a significant challenge. From a broader nonlinear-dynamics perspective, recurrence-plot analysis has been used to distinguish regular and chaotic behaviors in nonlinear mechanical systems, providing a complementary means of characterizing complex dynamic responses [13].

As a promising control paradigm, data-driven control approaches have recently attracted increasing attention in marine robotics. Before the emergence of modern data-driven methods, model-independent controllers such as proportional–integral–derivative (PID) control were widely adopted in practical USV applications because of their simple structure and ease of implementation. However, their performance is highly dependent on parameter tuning and often deteriorates under nonlinear dynamics and time-varying disturbances. Recent advances in data-driven control have introduced a variety of learning-based approaches [14]. Reinforcement learning (RL) [15,16] and deep deterministic policy gradient (DDPG) [17] directly learn control policies from interaction data, providing improved adaptability in complex environments. In addition, Gaussian Process (GP)-based methods [18], Koopman Operator (KO)-based methods [19], and Physics-Informed Neural Network (PINN)-based methods [20] exploit input–output data to capture system dynamics, thereby improving model accuracy and control performance. These approaches preserve certain model interpretability while reducing reliance on manually established models.

Recently, neural network-based data-driven control methods have emerged as promising approaches due to their powerful nonlinear approximation and learning capabilities [21]. By extracting dynamic characteristics from online measurements, neural networks can approximate unknown system dynamics and avoid reliance on prior physical models [22,23]. However, in practical applications, neural network-based methods inevitably suffer from residual approximation errors due to the continuously varying marine environment, which may further degrade the stability of the closed-loop control system. Therefore, developing a framework that ensures both learning capability and robust stability remains essential.

To enhance robustness against these learning errors and external disturbances, various robust control strategies, such as disturbance observer-based control [24], adaptive robust control [25], and Sliding Mode Control (SMC) [26], have been developed. Among them, SMC has attracted considerable attention because of its capability to compensate for residual learning errors and reject external disturbances, making it particularly suitable for neural network-based data-driven control [27]. By utilizing neural networks to learn dominant unknown dynamics from operational data, the SMC mechanism only compensates for remaining approximation errors and disturbances, thereby reducing the required switching gain and alleviating the chattering problem. Therefore, this study develops an RBF-SMC framework, where the RBF neural network serves as a data-driven dynamic estimator, while SMC provides robust regulation against learning errors and environmental disturbances.

Furthermore, practical USV operations often involve uncertain control effectiveness caused by variations in operating conditions, actuator characteristics, and system configurations. Such uncertainties may result in unknown control coefficients, posing significant challenges to stable and accurate heading control. The Nussbaum gain technique has been

widely recognized as an effective approach for addressing systems with unknown control coefficients by adaptively compensating for the uncertain input gain [28,29]. Therefore, the Nussbaum gain technique is incorporated into the proposed control framework in this paper to ensure the stability of heading tracking under uncertain control directions.

However, existing studies generally address unknown nonlinear dynamics, residual approximation errors, external disturbances, and unknown control coefficients separately. A unified data-driven control framework that simultaneously learns the unknown dynamics, compensates for the residual uncertainties, and accommodates the unknown control direction remains insufficiently investigated. The unresolved problem is therefore to achieve accurate USV heading tracking when the nonlinear dynamics, external disturbance, and control coefficient are unknown a priori, while simultaneously guaranteeing the boundedness of all closed-loop signals and the asymptotic convergence of the tracking error.

Motivated by the above observations, this paper proposes a novel data-driven Nussbaum-RBF Sliding Mode Control (NRSMC) framework for USV heading control under unknown USV system dynamics, uncertain control coefficients, and marine disturbances. The main contributions of this paper are summarized as follows:

(1) A novel data-driven Nussbaum-RBF Sliding Mode Control (NRSMC) scheme is proposed for USV heading control under unknown dynamics and disturbances. The RBF neural network is employed to learn unknown nonlinear system characteristics from online data, while the sliding mode mechanism improves robustness against approximation errors.
(2) An improved Nussbaum-type function is integrated to handle unknown control coefficients. Moreover, a boundary layer technique is introduced to alleviate chattering and enhance tracking performance.
(3) The effectiveness of the proposed NRSMC scheme is validated through comparative simulations and field experiments. The results demonstrate the improved heading tracking performance compared with NRABC in simulations and verify the stability and feasibility of the proposed controller in practical USV applications.

2. Preliminaries and Problem Formulation

2.1. Dynamic Representation of the USV

To formulate the heading control problem and facilitate stability analysis, the kinematic equations of an underactuated 3-DOF USV are briefly introduced [30].

$$\begin{cases} \dot{x} = u\cos\psi - v\sin\psi \\ \dot{y} = u\sin\psi + v\cos\psi \\ \dot{\psi} = r \end{cases} \tag{1}$$

The kinematics and dynamics of an underactuated USV are highly nonlinear and strongly coupled. For the purpose of heading control, by defining the state variables as $x_1 = \psi$ and $x_2 = r$, the heading control system can be abstracted into the following general nonlinear strict-feedback form [30]:

$$\begin{cases} \dot{x}_1 = x_2 \\ \dot{x}_2 = f(x_2) + b\sigma_r + d \end{cases} \tag{2}$$

where $f(x_2)$ represents the unknown nonlinear dynamics, b is the unknown control coefficient, and d denotes the unknown external environmental disturbances.

Earth-fixed frame ($O_e - X_eY_e$) and body-fixed frame ($O_b - X_bY_b$) are two coordinate systems to describe the motion of USVs [31], as shown in Figure 1.

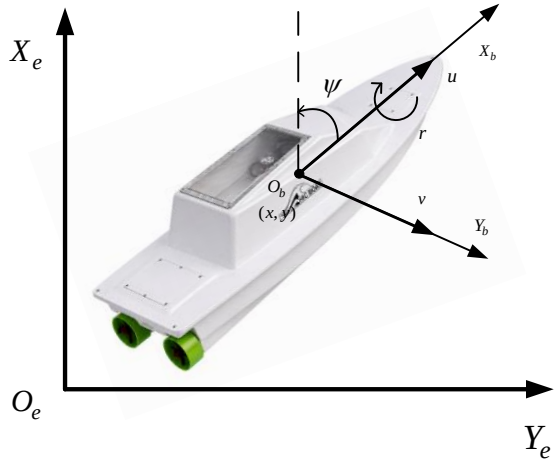


Figure 1. Earth-fixed and body-fixed coordinate systems of USV.

To design the USV heading controller, the following assumption is made for the system:

Assumption 1. *The external disturbances are time-varying, bounded, and slowly varying, satisfying* $0 < |d| < D < \infty$.

Remark 1. *The parameters influenced by the aquatic environment and the dynamic characteristics of the actuators may undergo significant variations, such as added mass and damping coefficients. This leads to uncertainty of* $f(x_2)$ *and signs of b, in Equation (2). Assumption 1 is valid as the energy associated with the forces generated by environmental disturbances acting on the USV is finite, and the frequency of these disturbances is significantly lower than the frequency of the vessel's inherent dynamics.*

2.2. RBF Neural Network

It is well established that RBF neural networks possess the universal approximation capability, enabling them to approximate any unknown continuous nonlinear function. This characteristic is particularly effective for addressing control problems characterized by unknown nonlinearities. Consequently, for the unknown nonlinear function $f(x_2)$ in Equation (2), this paper employs an RBF neural network to perform the estimation, thereby circumventing the complex procedures associated with system modeling and identification. The RBF neural network is defined as follows:

$$\begin{cases} f(x_2) = w^{*T} h(x) + \varepsilon \\ h_j = \exp\left(\frac{\|x_2 - c_j\|^2}{2b_j^2} \right) \end{cases} \tag{3}$$

where j denotes the j-th node in the hidden layer, and x_2 represents the input vector of the network. $h = [h_1, h_2, \ldots, h_n]^T$ is the output vector of the Gaussian functions; $c_j = [c_{j1}, c_{j2}, \ldots, c_{jm},]$ represents the center vector of the j-th neuron; and $b_j > 0$ denotes the width of the Gaussian function for the j-th hidden layer neuron. Furthermore, w^* represents the ideal weight vector of the network, and ε is the network approximation error, satisfying $|\varepsilon| \leq \varepsilon_N$, where $\varepsilon_N > 0$ is a constant. By taking x_2 as the network input and defining $\hat{w}$ as the estimated weight output of the RBF network, we obtain:

$$\hat{f}(x) = \hat{w}^T h(x) \tag{4}$$

2.3. Nussbaum Gain Control Technology

The problem of unknown control gains represents a significant challenge in control engineering. In USV systems, the uncertainty regarding control coefficients renders the controller design particularly complex. The Nussbaum gain technique is an effective approach for addressing the problem of unknown control coefficients. A Nussbaum-type function is defined as follows:

$$N(k) = k^2 \cdot \cos(k) \tag{5}$$

where k is a real number, and the function $N(k)$ satisfies the following bilateral properties [28]:

$$\begin{cases} \lim\limits_{k \to \pm\infty} \sup \frac{1}{k} \int_0^k N(s)ds = \infty \\ \lim\limits_{k \to \pm\infty} \inf \frac{1}{k} \int_0^k N(s)ds = -\infty \end{cases} \tag{6}$$

2.4. Control Objective

Assumption 2. *Assume the desired heading x_d and its first two derivatives are continuous and bounded.*

The tracking error $e = [e_1, e_2]^T$ is defined as shown in Equation (7). The control objective is to force the USV to track desired heading angle x_d, ensuring tracking error e_1 converges asymptotically to zero or a small residual set. Furthermore, the controller must guarantee global stability, ensuring all closed-loop signals remain bounded. The proposed control structure is illustrated in Figure 2.

$$\begin{cases} e_1 = x_1 - x_{1d} \\ e_2 = x_2 - x_{2d} \end{cases} \tag{7}$$

where $\dot{x}_{1d} = x_{2d}$. Taking the derivative of the above equation yields:

$$\begin{cases} \dot{e}_1 = \dot{x}_1 - \dot{x}_{1d} \\ \dot{e}_2 = \dot{x}_2 - \dot{x}_{2d} \end{cases} \tag{8}$$

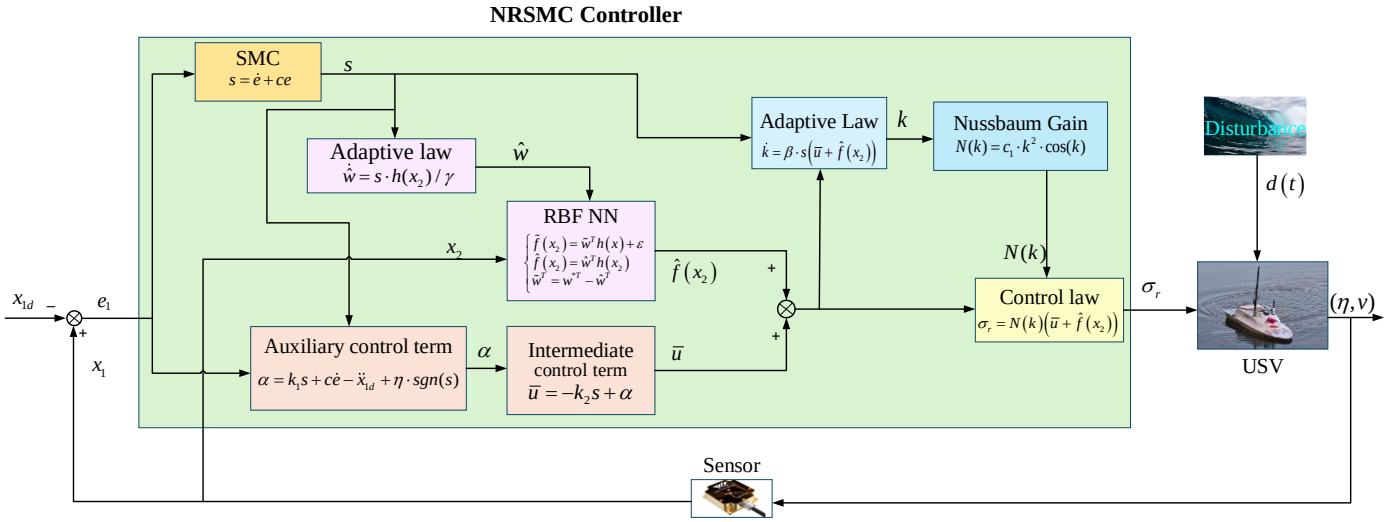


Figure 2. USV heading control block diagram.

Since the purpose of this paper is to achieve the desired heading tracking of the USV, from the above equation, a closed-loop tracking error system can be obtained:

$$\begin{cases} \dot{e}_1 = e_2 \\ \dot{e}_2 = f(x_2) + b\sigma_r + d(t) - \dot{x}_{2d} \end{cases} \tag{9}$$

Based on the formulation mentioned above, the control objective of this paper is established as follows: to design an effective yaw moment control input σ_r, that precisely regulates the heading motion of the USV, driving the actual heading angle x_1 to track the preset desired heading angle x_{1d} and satisfying the boundedness and asymptotic-convergence objectives stated above.

3. Controller Design

Aiming at precise heading regulation of USVs in complex disturbance environments, this paper proposes a robust control strategy based on NRSMC. First, to tackle the issue of unknown dynamics, an RBF neural network is employed to approximate the unknown system dynamics online. Adaptive laws are designed to adjust the network weights in real-time to ensure effective compensation. Then, regarding the problem of unknown control coefficients, an improved Nussbaum function and its parameter adaptive evolution laws are introduced.

Lemma 1 [32,33]**.** *Let $V(t)$ and $k(t)$ be smooth functions defined on the interval* [0,t_f), *with $V(t) \geq 0$. Let $N(\cdot)$ be a smooth Nussbaum-type function, and θ_0 be a non-zero constant. If the following condition is satisfied:*

$$V(t) \leq \int_0^t (\theta_0 N(k(\tau)) + 1)\dot{k}(\tau)d\tau + const\,, \forall\, t \in \left[0, t_f\right) \tag{10}$$

Then, $V(t)$, $k(t)$, and $\int_0^t (\theta_0 N(k(\tau)) + 1)\dot{k}(\tau)d\tau$ are bounded for all t∈[0,t_f).

Lemma 2 (Barbalat' Lemma) [34]**.** *If $f \in L_\infty$, $\dot{f} \in L_\infty$, and $f \in L_p$ with $p \in$ [1,∞), then $\lim_{t\to\infty} f(t) = 0$.*

First, the sliding surface is defined as follows:

$$s = \dot{e} + \mathrm{ce} \tag{11}$$

where $c > 0$.

$$\dot{s} = \text{-}\,\ddot{x}_{1d} + f(x_2) + b\sigma_r + d(t) + c\dot{e} \tag{12}$$

where σ_r denotes the control input, and the external disturbance satisfies $|d| \leq D$. Furthermore, an RBF neural network is utilized to approximate the unknown function $f(x_2)$, defined as follows:

$$\begin{cases} \widetilde{f}(x_2) = f(x_2) - \hat{f}(x_2) = \widetilde{w}^T h(x) + \varepsilon \\ \hat{f}(x_2) = \hat{w}^T h(x_2) \\ \widetilde{w}^T = w^{*T} - \hat{w}^T \end{cases} \tag{13}$$

where w^* denotes the ideal weight vector of the network, and ε represents the network approximation error, satisfying $|\varepsilon| \leq \varepsilon_N$. To ensure the stability of the system, the adaptive law for the neural network weight $\hat{w}$ is designed as follows:

$$\dot{\hat{w}} = s \cdot h(x_2)/\gamma \tag{14}$$

where $\gamma > 0$ is a constant. Let $\beta > 0$, $\eta > 0$, and $k_1 > k_2 > 0$. The control law is designed as follows:

$$\sigma_r = N(k)\left(\overline{u} + \hat{f}(x_2)\right) \tag{15}$$

To address the unknown control direction, the actual control input σ_r employs the Nussbaum function $N(k)$ to scale the composite signal formed by $\overline{u}$ and the RBF neural network.

Therefore, this paper proposes an improved Nussbaum function, where $c_1 > 0$ is a designed parameter, defined as follows:

$$N(k) = c_1 \cdot k^2 \cdot \cos(k) \tag{16}$$

The Nussbaum gain adaptation law $\dot{k}$ is as follows:

$$\dot{k} = \beta \cdot s\left(\overline{u} + \hat{f}(x_2)\right) \tag{17}$$

where $\overline{u}$ is synthesis of the intermediate control signal based on α and s.

$$\overline{u} = -k_2 s + \alpha \tag{18}$$

where α serves as an auxiliary control term incorporating the sliding mode switching law $\eta sgn(s)$ to enhance robustness against disturbances.

$$\alpha = k_1 s + c\dot{e} - \ddot{x}_{1d} + \eta \cdot \mathrm{sgn}(s) \tag{19}$$

4. Closed-Loop Stability Analysis

To implement precise heading tracking for the USV subject to unknown dynamics and uncertain control coefficients, the Nussbaum-RBF sliding mode controller is designed using (14)–(19). Within this framework, the stability of the closed-loop system is analyzed. The convergence of the tracking error and the boundedness of closed-loop signals can be stated in the following part.

Theorem 1. *Consider the closed-loop USV heading control system composed of the system dynamics (9), the RBF neural network approximation (13), and the adaptive control law (15) with update laws (14) and (17). Specifically, the heading tracking error $e(t)$ and its derivative $\dot{e}(t)$ converge to zero asymptotically as $t \to \infty$, while all other closed-loop signals remain bounded.*

Proof of Theorem 1. Choose the Lyapunov function as:

$$V = \frac{1}{2}s^2 + \frac{1}{2}\gamma\tilde{w}^T\tilde{w} \tag{20}$$

Differentiating V with respect to time yields:

$$\dot{V} = s\dot{s} - \gamma\tilde{w}^T\dot{\hat{w}} \tag{21}$$

Substitute (12) and (13) into the above equation:

$$\dot{V} = s\left(-\ddot{x}_{1d} + w^{*T}h(x_2) + \varepsilon + b\sigma_r + d + c\dot{e}\right) - \gamma\tilde{w}^T\dot{\hat{w}} \tag{22}$$

Substituting Equation (19) into the above equation, we obtain:

$$\dot{V} = s(\alpha - k_1 s - \eta \cdot \mathrm{sgn}(s) + w^{*T}h(x_2) + \varepsilon + b\sigma_r + d) - \gamma\tilde{w}^T\dot{\hat{w}} + \frac{\dot{k}}{\beta} - \frac{\dot{k}}{\beta} \tag{23}$$

where $\eta \geq \varepsilon_N + D$. Consequently, it follows that $[d(t) + \varepsilon]s - \eta\,|s| \leq 0$. Substituting $\frac{\dot{k}}{\beta} = s(\overline{u} + \hat{f}(x_2))$ into the above inequality yields:

$$\begin{aligned} \dot{V} &\leq s(\alpha - k_1 s + b\sigma_r) + s w^{*T} h(x_2) - \gamma \tilde{w}^T \dot{\hat{w}} + \frac{\dot{k}}{\beta} - s(-k_2 s + \alpha + \hat{f}(x_2)) \\ &= (k_2 - k_{1'})s^2 + (\mathrm{bN}(k) + 1)\frac{\dot{k}}{\beta} + \tilde{w}^T\left(s \cdot h(x_2) - \gamma \dot{\hat{w}}\right) \end{aligned} \tag{24}$$

And substituting the adaptive law (14), yields $sh(x_2) + \gamma\dot{\hat{w}} = 0$.

Integrating both sides of the above equation from 0 to t, we obtain:

$$\begin{aligned} V(t) - V(0) &\leq \int_0^t \frac{1}{\beta}(b \cdot N(k(\tau)) + 1)\dot{k}(\tau)d\tau + \int_0^t (k_2 - k_1)s^2(\tau)d\tau \\ V(t) - \int_0^t (k_2 - k_1)s^2(\tau)d\tau &\leq \int_0^t \frac{1}{\beta}(b \cdot N(k(\tau)) + 1)\dot{k}(\tau)d\tau + V(0) \end{aligned} \tag{25}$$

According to Lemma 1, it can be concluded that $V(t) - \int_0^t (k_2 - k_1)s^2(\tau)d\tau$ is bounded. The term involving $\dot{k}$ is bounded. Consequently, $V(t)$ is bounded, implying $s \in L_\infty$ and $\widetilde{w} \in L_\infty$. From the definition of V, we also have $s \in L_2$ since $\int_0^\infty s^2(\tau)d\tau < \infty$.

Since all signals in the closed-loop system are bounded, the derivative of the sliding surface $\dot{s}$ is bounded, which implies that s(t) is uniformly continuous. According to Lemma 2, for a uniformly continuous function s(t), if $s \in L_2$, then $\lim_{t\to\infty} s(t) = 0$. Therefore, from (11), we can obtain:

$$\dot{e} + ce = 0 \tag{26}$$

The solution to the above equation is

$$e(t) = e(0)e^{-ct} \tag{27}$$

Consequently, it can be concluded that the tracking error and its derivative converge to zero asymptotically, i.e., $\lim_{t\to\infty} e(t) = 0$ and $\lim_{t\to\infty} \dot{e}(t) = 0$. Thus, asymptotic convergence of the tracking control is achieved. □

5. Simulation and Analysis

In this section, a simulation environment is established, and simulations are conducted to verify the performance of the proposed strategy, particularly its transient and steady-state performance in both heading keeping and tracking tasks.

5.1. The Simulation Environment and Parameter Settings

The simulation environment is established using MATLAB/Simulink (Version R2023b, MathWorks, Natick, MA, USA). The controlled USV model and its associated hydrodynamic parameters employed in the simulations were adopted from Gonzalez-Garcia and Castañeda [30]. Furthermore, to simulate environmental uncertainties, a second-order wind-wave system is introduced, utilizing Gaussian white noise as the disturbance term. This disturbance model is formulated as follows [35]:

$$h(\omega) = \frac{0.4198\omega}{\omega^2 + 0.3638\omega + 0.3675} \tag{28}$$

This section presents a comparative analysis between the proposed strategy and an NRABC scheme adopted from Wang et al. [36]. And the initial values of the USV state variables are set as $\eta(0) = [0,0,0]^T$ and $v(0) = [0,0,0]^T$.

Remark 2. *To mitigate performance degradation induced by chattering, the boundary layer technique is implemented. The switching term sgn(s) in Equation (19) is replaced by a smooth tanh(s/c_2) function. It is noteworthy that this substitution does not invalidate the preceding stability proof [37]. The boundary-layer function smooths the continuous sliding-mode control command but does not eliminate the discrete fluctuations caused by integer PWM quantization. Additionally, regarding the comparative NRABC strategy, parameter retuning is performed to accommodate the specific control plant used in this study.*

5.2. Case 1. The Desired Heading Angle Is Constant

To validate the heading keeping capability under dynamic environments, the simulation is conducted with a constant desired heading angle. The desired heading angle is set to x_d = 0.4 rad, with a simulation duration of 30 s. For the controller setup, the RBF neural network within the proposed NRSMC strategy consists of 1 input node, 5 hidden neurons, and 1 output node. The comparative NRABC utilizes an identical neural network structure, with all relevant parameter settings detailed in Table 1. Finally, Figure 3 and Table 2 respectively present the performance comparison between the proposed NRSMC and the NRABC in this USV heading–keeping task.

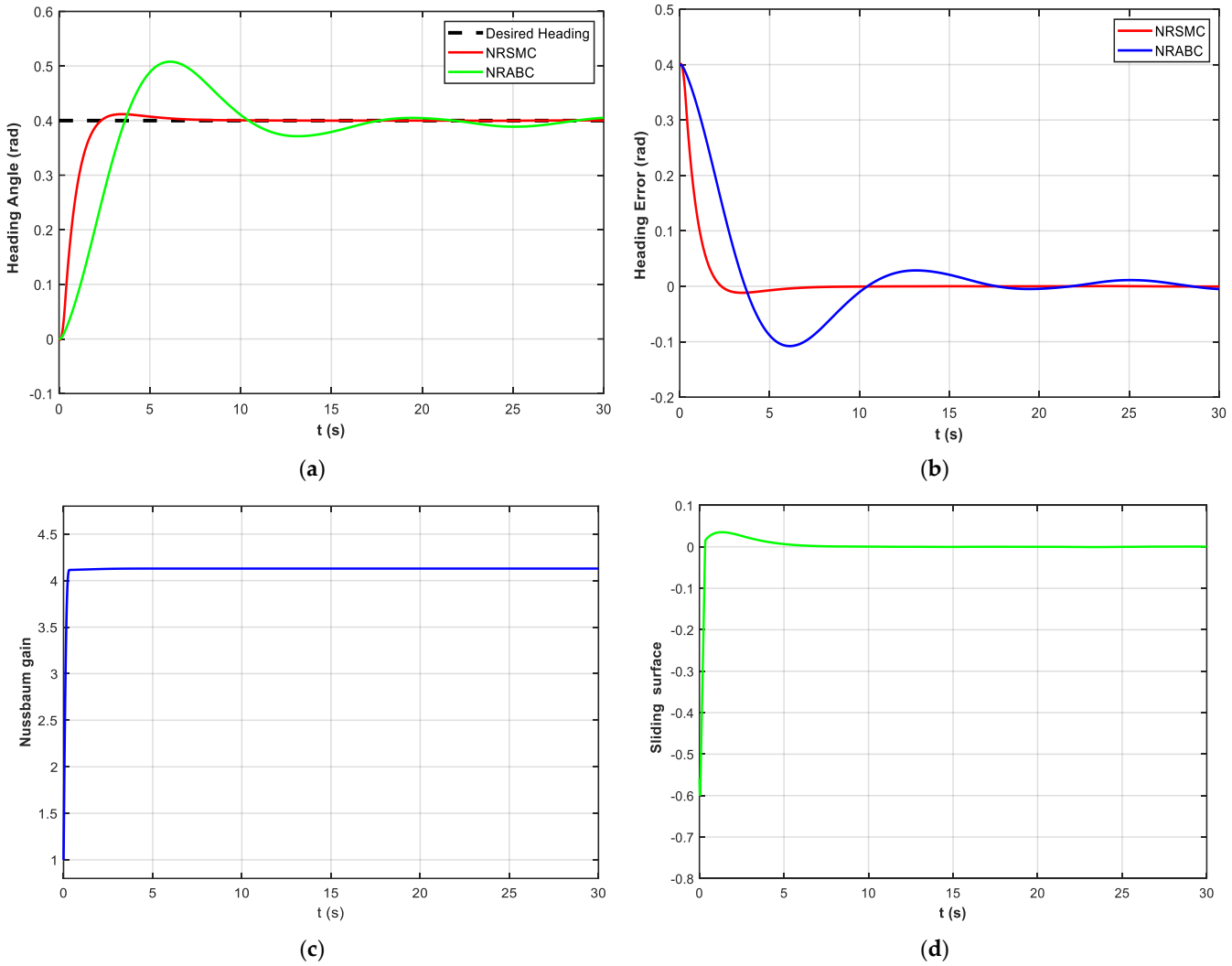


Figure 3. Simulation results for Case 1. (**a**) Comparison of the heading angle. (**b**) Comparison of tracking errors. (**c**) The trajectory of Nussbaum gain in NRSMC. (**d**) The trajectory of the sliding surface.

Table 1. Parameters of Case 1 and Case 2.

Item	Case 1	Case 2
RBFNN	$c_j = [-5, -2.5, 0, 2.5, 5]$, $b_j = 2$, $\hat{w} = 0$, $\gamma = 0.2$	$c_j = [-5, -2.5, 0, 2.5, 5]$, $b_j = 2$, $\hat{w} = 0$, $\gamma = 0.2$
Nussbaum gain	$c_1 = 4.2$, $k(0) = 1.55$, $\beta(0) = 5$.	$c_1 = 4.2$, $k(0) = 1.0$, $\beta(0) = 5$
NRSMC	$c = 0.9$, $c_2 = 2.05$, $\eta = 150$, $k_1 = 1$, $k_2 = 61$	$c = 1.4$, $c_2 = 4$, $\eta = 300$, $k_1 = 1$, $k_2 = 11$
NRABC	$\delta_1 = \delta_2 = 0.1$, $k_1 = 0.2$, $k_2 = 100$, $\Pi_1 = \Pi_2 = 0.1I_5$, $\hat{w}_1(0) = \hat{w}_2(0) = 0$	$\delta_1 = \delta_2 = 0.1$, $k_1 = 4$, $k_2 = 6$, $\Pi_1 = \Pi_2 = 0.1I_5$, $\hat{w}_1(0) = \hat{w}_2(0) = 0$

Table 2. Quantitative comparison of USV heading keep.

Item	Overshoot (%)	Settling Time (s)	RMSE	Steady-State Error
NRSMC	2.939%	4.810	0.053628	0.000445
NRABC	26.982%	26.679	0.094036	0.002925

To improve the reproducibility of the controller implementation and clarify the distinct roles of the RBF learning rate γ and the sliding-mode switching gain η, their engineering tuning and coordination procedure is described as follows. The learning rate γ and switching gain η should not be increased simultaneously. γ is first increased within a conservative range until the dominant unknown dynamics are learned without oscillatory weight updates. η is then selected to retain the robustness margin required for the remaining approximation error and disturbance. Excessive γ may amplify noise and transient overshoot, whereas excessive η increases switching activity; the preferred pair is therefore the smallest η that preserves robustness after satisfactory RBF adaptation has been obtained.

Table 2 shows that the proposed NRSMC achieves superior tracking performance over the NRABC, with lower overshoot (2.939% vs. 26.982%), shorter settling time (4.810 s vs. 26.679 s), and reduced RMSE. The improved performance is attributed to the RBF-based online dynamic learning and sliding mode regulation, which effectively handle unknown dynamics and disturbances. Moreover, the bounded Nussbaum gain and fast convergence of the sliding surface verify the effectiveness of the proposed adaptive mechanism.

5.3. Case 2. The Desired Heading Angle Is Time-Varying

To evaluate the tracking capability under dynamic conditions, the desired heading is set to a sinusoidal signal $x_d = 0.2\sin(t)$. The structure of the RBF neural network remains consistent with Case 1. The relevant controller parameters are shown in Table 1. The corresponding results are depicted in Figure 4 and Table 3.

Figure 4a visually illustrates the tracking performance of the two strategies. The trajectory of the proposed NRSMC almost perfectly coincides with the desired path. In contrast, the NRABC exhibits significant phase lag and amplitude attenuation at the peaks and troughs. As quantified in Table 3 and Figure 4b, the proposed NRSMC significantly outperforms the NRABC in tracking accuracy. While the NRABC suffers from substantial periodic oscillations (Max Error: 0.0765 rad), the NRSMC restricts the error to a minimal range (Max Error: 0.0165 rad). Furthermore, it achieves an order-of-magnitude reduction in RMSE (0.0020 vs. 0.0237) and steady-state error (0.0011 vs. 0.0129), demonstrating superior robustness against persistent disturbances. Finally, Figure 4c,d confirm internal stability; the Nussbaum gain dynamically adjusts and remains bounded within [2.0, 2.5], while the sliding surface rapidly converges to zero.

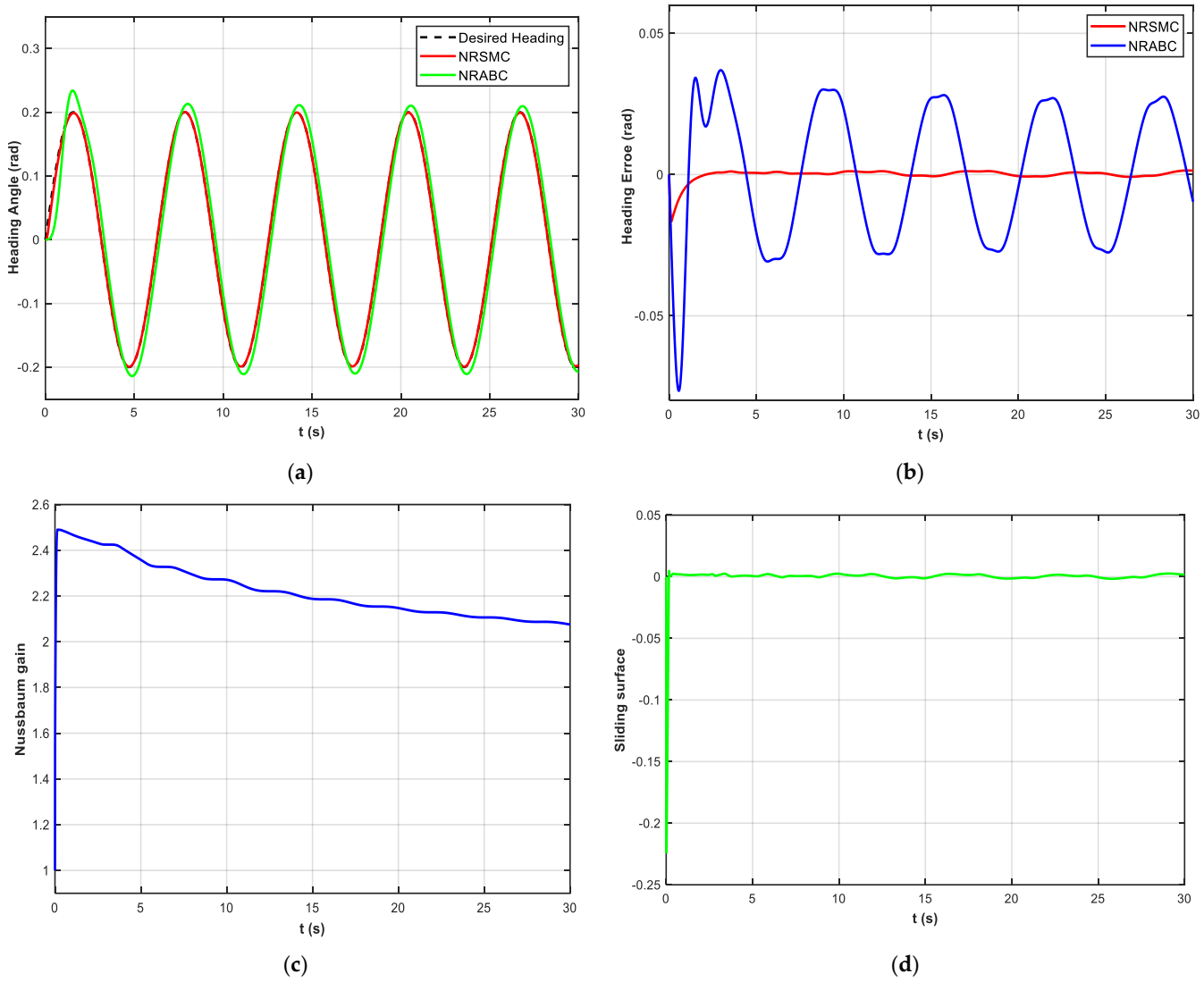


Figure 4. Simulation results for Case 2. (**a**) Comparison of the heading angle. (**b**) Comparison of tracking errors. (**c**) The trajectory of Nussbaum gain in NRSMC. (**d**) The trajectory of the sliding surface.

Table 3. Quantitative comparison of USV heading tracking.

Item	RMSE	Max Error	Steady-State Error
NRSMC	0.002025	0.016545	0.001142
NRABC	0.023715	0.076574	0.012923

In summary, the simulation results verify the effectiveness of the proposed NRSMC scheme in improving USV heading control performance. By combining RBF-based online dynamic learning with sliding mode robust regulation, the proposed method achieves accurate tracking without requiring complete prior knowledge of system dynamics and control gains. Compared with the NRABC, the NRSMC provides faster convergence, smaller tracking errors, and stronger robustness against disturbances. Moreover, the boundary layer technique effectively reduces chattering, enhancing the practical applicability of the proposed controller for USV systems.

6. Experiment and Analysis

To further validate the control performance and engineering practicality of the proposed NRSMC in actual navigation scenarios, an experimental platform was established based on a self-developed small-scale USV. Field trials were conducted at Haiyun Lake, Jiangsu University of Science and Technology, under conditions of a slight northwest breeze (approximately Force 1 on the Beaufort scale). The proposed control algorithm was implemented using Python (version 3.10) and deployed onto the USV's onboard control system.

6.1. Hardware Architecture

The small-scale USV employed in this study has a mass of 5.5 kg and a length of approximately 1.0 m. A lightweight design was adopted to accommodate experimental scenarios in nearshore shallow waters. The hardware system utilizes a Raspberry Pi 3B development board as the core control unit. Possessing multi-interface expansion capabilities and real-time data processing performance, this unit executes core functions including sensor data acquisition, control algorithm computation, and actuator command distribution.

Regarding the propulsion system, the USV is equipped with two DC propulsion motors arranged in a twin-motor differential steering configuration. Precise control of the heading attitude is achieved by regulating the rotational speed difference between the two motors. For the attitude perception module, a high-performance Inertial Measurement Unit (IMU) was selected. This sensor acquires the USV's three-dimensional attitude information (yaw, pitch, and roll) and angular velocities data in real-time. Specifically, the heading angle (yaw) and yaw rate serve as the core feedback signals for the heading control algorithm, providing critical state inputs for closed-loop control.

Based on the USV hardware platform and the proposed heading control Strategy mentioned above, the Raspberry Pi 3B core control unit computes the required yaw moment to satisfy the heading tracking requirements. Subsequently, this moment signal is converted into Pulse Width Modulation (PWM) control values. These PWM signals are transmitted directly via the General-purpose Input/Output (GPIO) pins of the Raspberry Pi to the Electronic Speed Controllers (ESCs). Consequently, precise regulation of the thrust generated by the two DC motors is achieved by adjusting the ESC outputs.

It is noteworthy that this USV is not equipped with an additional dedicated Microcontroller Unit (MCU). Instead, the Raspberry Pi directly undertakes the functions of PWM signal generation and output to complete the closed-loop control of the motors. The overall structure of the experimental platform is illustrated in Figure 5.

According to the literature by Ye et al. [38], the relationship between thrust, torque and the PWM wave is as follows:

$$T_{pwm} = \frac{T_N}{T_{max}} \times 30 + 76 \tag{29}$$

where T_{pwm} denotes the calculated PWM value, T_N represents the desired thrust for each thruster, and T_{max} indicates the maximum thrust capacity of each thruster.

Remark 3. *A critical procedure in this experiment involves converting the control torque computed by the controller into PWM signals. Given that this study focuses on the heading control of the USV, the surge speed of the vehicle was maintained at a constant 0.25 m/s throughout the experiment. Correspondingly, the baseline PWM value for each propulsion motor was set to 80 µs.*

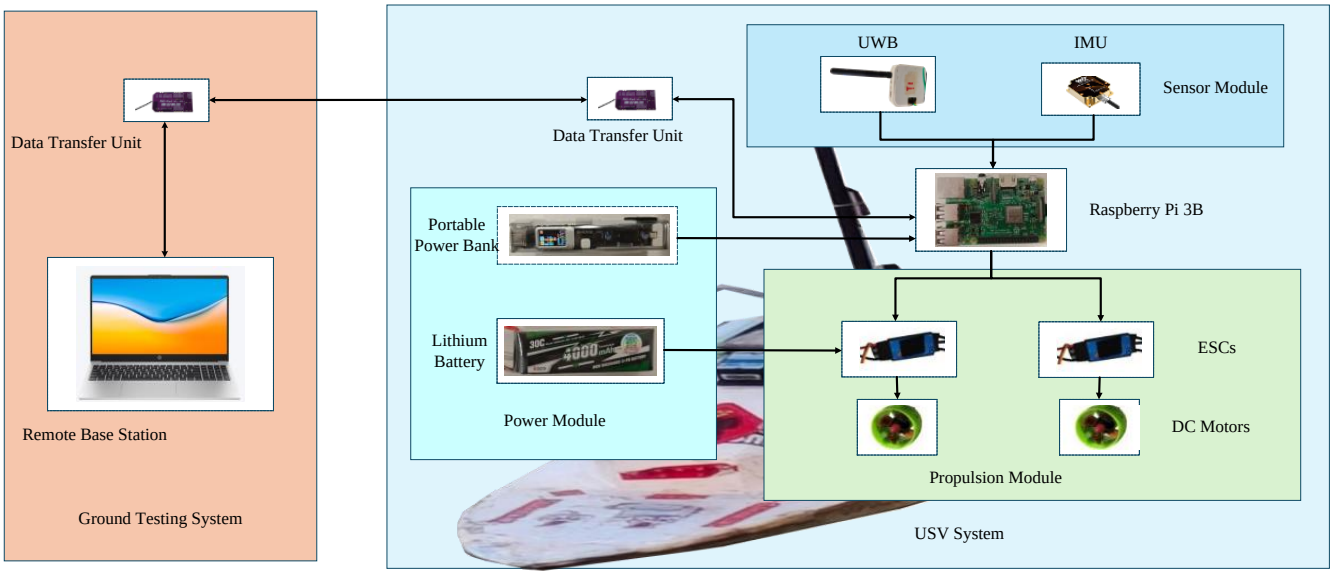


Figure 5. The structure of experimental platform.

6.2. Experimental Results

Based on the aforementioned USV platform, tracking experiments for both constant and curvilinear heading angles were conducted using the NRSMC scheme.

6.2.1. Case 1. The Desired Heading Angle Is Constant

In this experiment, the desired heading angle was set to 0.8 rad, with the initial system states initialized as $x_1(0) = -0.5$ rad and $x_2(0) = 0$. Upon receiving the yaw command, the heading angle gradually transitioned from -0.5 rad to 0.8 rad. The heading angle reached the desired value after approximately 10 s and was maintained stably thereafter, as illustrated in Figure 6a.

The initial value of the Nussbaum gain was set to 1.5, and it reached a steady value after approximately 1.7 s. Figure 6b depicts the evolution process of k. Figure 6c illustrates the variations in the thrust of the two motors during the control process. It is noteworthy that, due to hardware limitations, the PWM values for the motors must be integers. Consequently, this quantization constraint may lead to a certain deviation between the actual motor thrust and the theoretical value.

Although the chattering phenomenon is inherent to SMC upon reaching the sliding surface, the boundary layer technique employed in the proposed controller effectively attenuated this chattering. The evolution of the sliding surface is shown in Figure 6d. During the navigation of the USV, once the heading angle reached the target value, the yaw moment τ_r remained substantially constant, and $N(k)$ remained invariant, allowing the USV to maintain a straight course. This demonstrates that the Nussbaum function effectively resolved the problem of unknown control direction in practical USV heading control.

6.2.2. Case 2. The Desired Heading Angle Is Time-Varying

In this experiment, the desired heading angle was set to $x_d = 0.4\sin(0.25t)$rad, with the initial system states initialized as $x_1(0) = -0.15$ rad, $x_2(0) = 0$. Upon activation, the USV heading successfully converged to the reference angle, as illustrated in Figure 7a. Although a slight phase lag is observed, it may result from the sampling interval and data-transmission latency. Theorem 1 does not include communication delay and therefore provides no formal admissible-delay bound. Thus, the present experiment demonstrates only empirical tolerance to the small latency of the current platform, rather than a general

delay-robustness guarantee. For larger or time-varying delays, delay-aware prediction or predictor-based compensation should be considered.

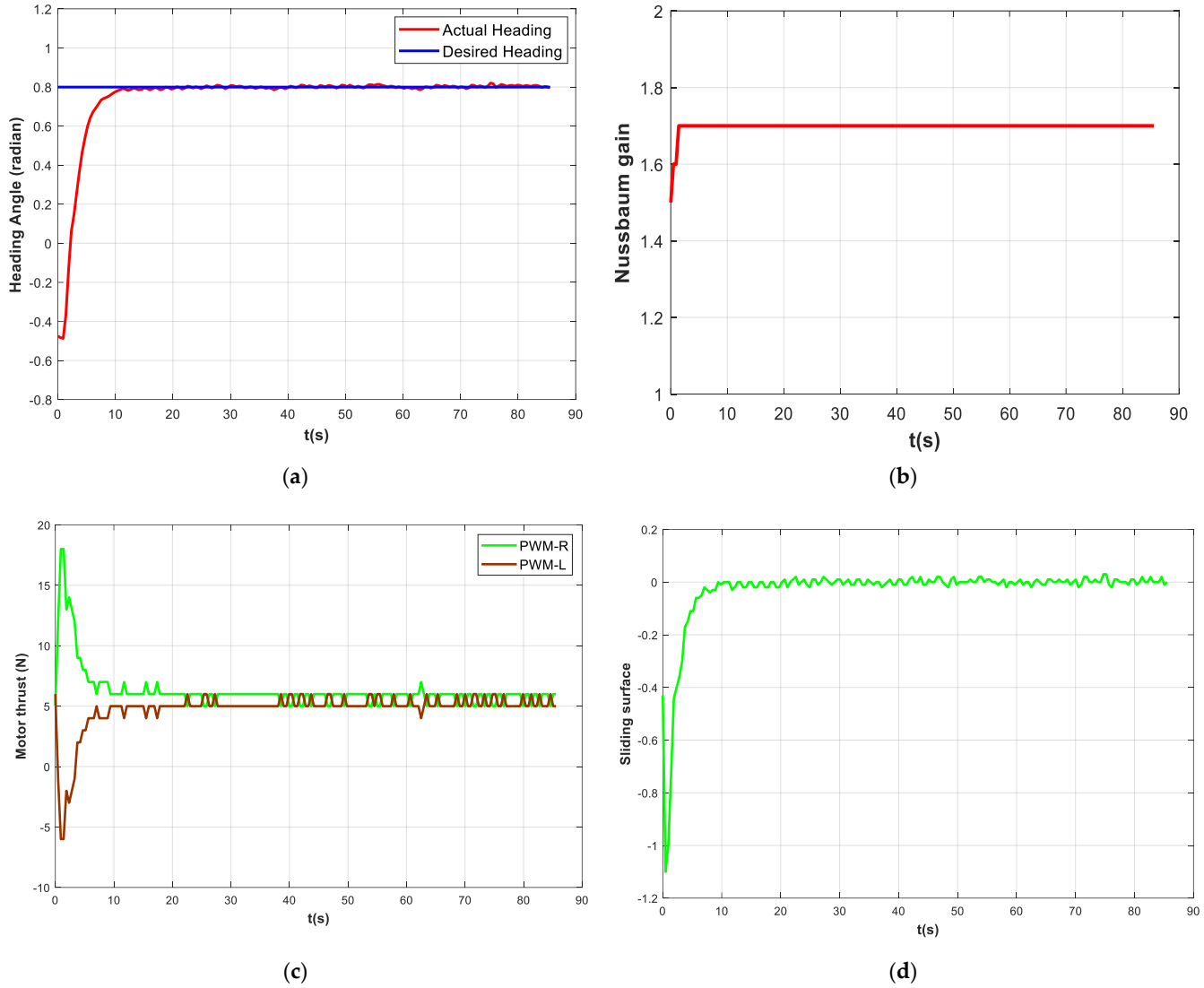


Figure 6. Experimental results for Case 1. (**a**) Straight-line heading angle tracking. (**b**) The trajectory of Nussbaum gain. (**c**) The changes in thrust PWM. (**d**) The trajectory of the sliding surface.

The initial value of the Nussbaum gain was set to 1.5. As shown in Figure 7b, the gain k underwent a step-wise adaptation to accommodate the changing dynamics and unknown control direction, eventually stabilizing at approximately 1.7 after 30 s. Figure 7c illustrates the periodic variations in the thrust PWM signals of the two motors. The control inputs vary continuously to generate the alternating yaw moment required for sinusoidal motion. Consistent with the previous case, the hardware constraint requiring integer PWM values may introduce minor deviations between the theoretical and actual motor thrust.

The thrust variations shown in Figure 7c indicate that smoothing the continuous switching law does not completely eliminate the fluctuations introduced by integer PWM quantization. For subsequent hardware implementation, the recommended actuator-interface sequence is continuous controller output–slew-rate limitation–amplitude saturation–integer PWM quantization–motor driver. The slew-rate limiter bounds the command increment at each sampling instant, while its rate limit should be selected by balancing actuator protection and command smoothness against the additional tracking delay. The field data reported in this study were collected without such a limiter; therefore,

no experimentally verified reduction in PWM fluctuation, motor loss, or actuator wear is claimed.

Furthermore, the evolution of the sliding surface is depicted in Figure 7d. Unlike the straight-line case where s converges to zero, the sliding variable here oscillates within a bounded region due to the time-varying nature of the reference signal. However, the employed boundary layer technique effectively suppresses high-frequency chattering, ensuring that the control action remains smooth and the system remains stable.

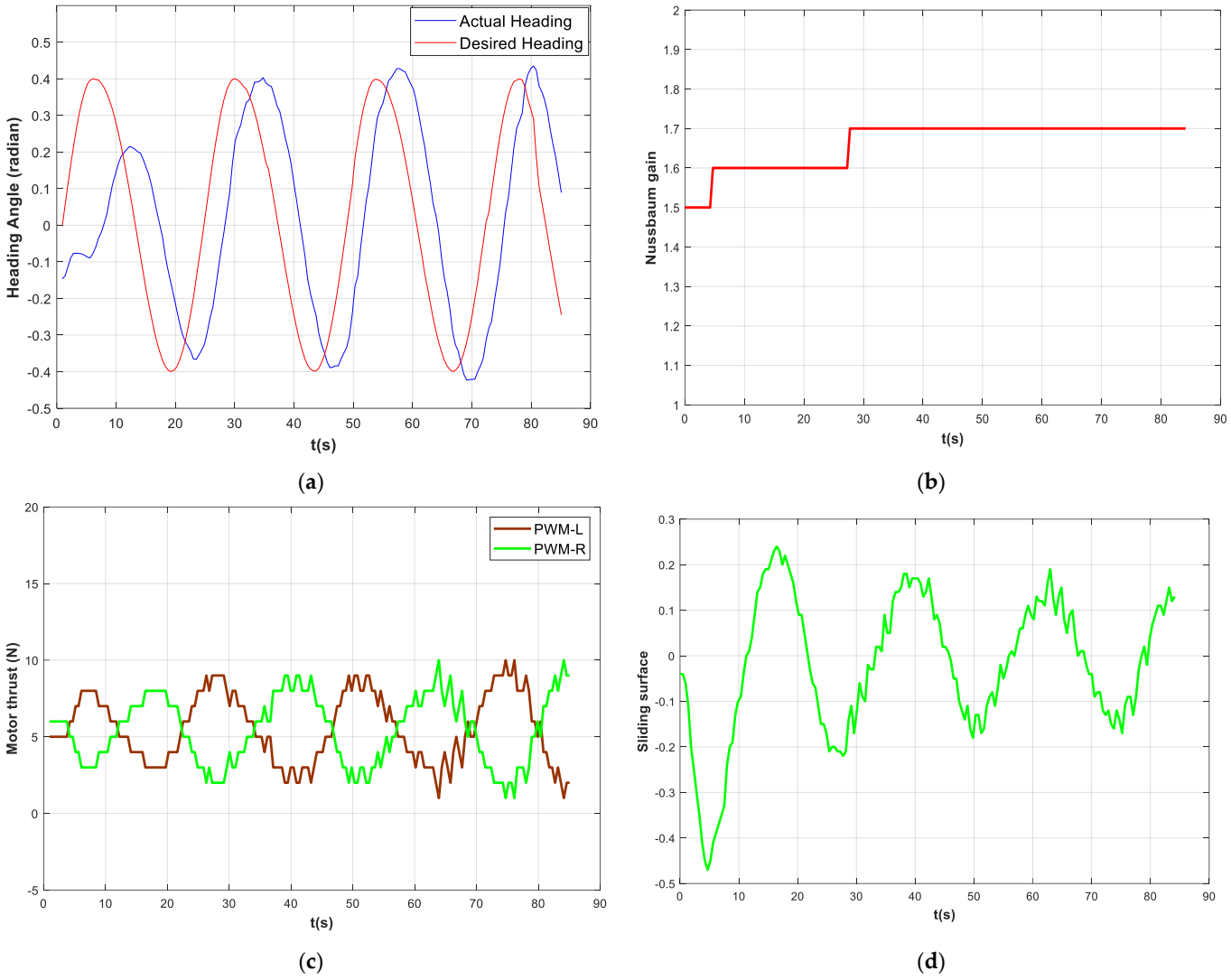


Figure 7. Experimental results for Case 2. (**a**) Sinusoidal heading angle tracking. (**b**) The trajectory of Nussbaum gain for the sinusoidal heading angle. (**c**) The changes in thrust PWM for the sinusoidal heading angle. (**d**) The trajectory of the sliding surface for the sinusoidal heading angle.

7. Conclusions

This paper investigated the heading control problem of underactuated USVs subject to unknown dynamics, external disturbances, and uncertain control coefficients. A novel data-driven Nussbaum-RBF Sliding Mode Control (NRSMC) framework was proposed to enhance adaptability and robustness under uncertain marine conditions. In this framework, the RBF neural network was employed to learn unknown nonlinear dynamic characteristics from online measurements, reducing the dependence on accurate mathematical models. Meanwhile, the sliding mode mechanism was introduced to improve robustness against approximation errors and disturbances, while the Nussbaum gain technique was integrated

to address uncertain control coefficients. A boundary layer method was further adopted to alleviate chattering and improve practical applicability.

On this basis, the proposed framework was evaluated through stability analysis, comparative simulations, and field experiments. The stability of the closed-loop system s analyzed using the Lyapunov–Nussbaum approach. Compared with NRABC, the proposed NRSMC reduced the settling time by 81.96% and the overshoot by 89.11% in the constant-heading test. In the sinusoidal tracking test, the RMSE, maximum tracking error, and SSE were reduced by 91.46%, 78.39%, and 91.16%, respectively. Finally, field experiments on a self-developed USV platform further verified the effectiveness and engineering feasibility of the proposed data-driven control framework.

To further examine possible improvements in error-convergence speed, a finite-time extension was also investigated. A finite-time sliding manifold can be incorporated into the proposed framework while retaining the RBF approximation and Nussbaum mechanism. Matched step and sinusoidal simulations showed only modest changes in tracking performance, together with small trade-offs in overshoot, phase lag, and control effort. Since this study focuses on the integrated treatment of unknown nonlinear dynamics and unknown control direction, the original linear manifold and stability proof are retained; a rigorous finite-time reformulation is left for future work.

Author Contributions: All authors contributed to the study conception and design. J.Z.: Writing—original draft, Conceptualization, Methodology, Formal analysis and Validation. Y.D.: Data curation, Software, Investigation and Resources. W.X.: Writing—review & editing and Visualization. W.L.: Supervision, Project administration and Funding acquisition. All authors have read and agreed to the published version of the manuscript.

Funding: This work was supported by the Postgraduate Research & Practice Innovation Program of Jiangsu Province [Grant KYCX25_4337], the Jiangsu Province Higher Education Basic Science (Natural Science) Research Project [Grant 23KJD120004], and the Research Startup Foundation of Jiangsu University of Science and Technology [Grant 1032932006].

Institutional Review Board Statement: Not applicable

Informed Consent Statement: Not applicable

Data Availability Statement: The original contributions presented in this study are included in the article. Further inquiries can be directed to the corresponding author.

Acknowledgments: During the preparation of this work, the authors used Gemini 3.6 and ChatGPT (GPT-4) (OpenAI) and Grammarly solely to improve grammar, clarity, and readability. After using this tool, the authors reviewed and edited the content as needed and take full responsibility for the content of this publication.

Conflicts of Interest: The authors declare no conflicts of interest.

References

1. Wu, S.; Ye, H.; Liu, W.; Yang, X.; Liu, Z.; Zhang, H. An Improved ELOS Guidance Law for Path Following of Underactuated Unmanned Surface Vehicles. *Sensors* **2024**, *24*, 5384. [CrossRef] [PubMed]
2. Yan, X.; Yang, X.; Feng, B.; Liu, W.; Ye, H.; Zhu, Z.; Shen, H.; Xiang, Z. A navigation accuracy compensation algorithm for low-cost unmanned surface vehicles based on models and event triggers. *Control Eng. Pract.* **2024**, *146*, 105896. [CrossRef]
3. Zheng, H.; Liu, C. An overview of unmanned surface vehicles: Methods, practices, and applications. *Control Eng. Pract.* **2025**, *164*, 106479. [CrossRef]
4. He, Z.; Fan, Y.; Wang, G.; Qiao, S. Finite time course keeping control for unmanned surface vehicles with command filter and rudder saturation. *Ocean Eng.* **2023**, *280*, 114403. [CrossRef]
5. Yu, J.; Wei, Y.; Chen, Y.; Zhang, H.; Xu, J.; Zhao, Z. U-control-based active disturbance-rejection control revealed by the sliding mode for USV heading control. *Control Eng. Pract.* **2025**, *159*, 106288. [CrossRef]

6. Li, Z.; Xie, S.; Ning, J.; Hu, X.; Wang, K. Event-triggered adaptive heading control for unmanned surface vehicles with input quantification and disturbance observer. *Ocean Eng.* **2025**, *341*, 122657. [CrossRef]
7. Wu, N.; Fan, Y.; Wang, R.; Wang, M.; Wu, C.; Wang, Y. Development and field testing of an unmanned surface vehicle system for guidance control and target tracking. *Ocean Eng.* **2025**, *316*, 119924. [CrossRef]
8. Zhao, Y.; Zhang, Z.; Wang, J.; Wang, H. Fin-rudder joint control based on improved linear-quadratic-regulator algorithm. *IEEE Access* **2022**, *10*, 111105–111114. [CrossRef]
9. Hong, L.; Liu, H.; Yang, Q.; Yao, J. Model predictive attitude control of unmanned surface vehicle based on short-time wave prediction. *Ocean Eng.* **2024**, *314*, 119727. [CrossRef]
10. Li, X.C.; Gonzalez-Garcia, A.; Castañeda, H. Optimizing unmanned surface vehicle control: A data-enabled learning approach. *Control Eng. Pract.* **2026**, *168*, 106737. [CrossRef]
11. Li, J.; Fan, Y. Fixed-time event-triggered fault-tolerant formation-containment control for underactuated USVs with uncertain dynamics. *Nonlinear Dyn.* **2025**, *113*, 21435–21454. [CrossRef]
12. Dong, Z.; Tan, F.; Zhou, W.; Wang, B.; Liu, Y. Distributed formation control of underactuated UMVs based on nonlinear model prediction algorithm with obstacle avoidance strategy incorporating relative velocity constraints. *Ocean Eng.* **2024**, *312*, 119272. [CrossRef]
13. Gupta, M.; Sharma, P.; Mondal, A.K.; Kumar, A. Visual Recurrence Analysis of Chaotic and Regular Motion of a Multiple Pendulum System. *Arab. J. Sci. Eng.* **2017**, *42*, 2711–2716. [CrossRef]
14. Hong, L.; Liu, L.; Peng, Z.; Zhang, F. Control of marine robots in the era of data-driven intelligence. *Annu. Rev. Control Robot. Auton. Syst.* **2025**, *9*, 243–272. [CrossRef]
15. Liu, Z.; Zhang, Q.; Xiang, X.; Yang, S.; Huang, Y.; Zhu, Y. Intelligent decision and planning for unmanned surface vehicle: A review of machine learning techniques. *Ocean Eng.* **2025**, *327*, 120968. [CrossRef]
16. Lou, M.; Yang, X.; Hu, J.; Zhu, Z.; Shen, H.; Xiang, Z.; Zhang, B. A balanced collision avoidance algorithm for USVs in complex environment: A deep reinforcement learning approach. *IEEE Trans. Intell. Transp. Syst.* **2024**, *25*, 21404–21415. [CrossRef]
17. Wang, Y.; Zhao, S.; Wang, Q. Cooperative control of velocity and heading for unmanned surface vessel based on twin delayed deep deterministic policy gradient with an integral compensator. *Ocean Eng.* **2023**, *288*, 115943. [CrossRef]
18. Li, F.; Li, H.; Wu, C. Gaussian process based learning model predictive control with application to USV. *IEEE Trans. Ind. Electron.* **2024**, *71*, 16388–16397. [CrossRef]
19. Rahmani, M.; Redkar, S. Enhanced Koopman operator-based robust data-driven control for 3 degree of freedom autonomous underwater vehicles: A novel approach. *Ocean Eng.* **2024**, *307*, 118227. [CrossRef]
20. Liu, T.; Zhao, J.; Huang, J.; Li, Z.; Xu, L.; Zhao, B. Research on model predictive control of autonomous underwater vehicle based on physics informed neural network modeling. *Ocean Eng.* **2024**, *304*, 117844. [CrossRef]
21. Ma, Y.; Shi, Y.; Jiang, C. A Discrete-Form Double-Integration-Enhanced Recurrent Neural Network for Stewart Platform Control with Time-Varying Disturbance Suppression. *Informatics* **2026**, *13*, 49. [CrossRef]
22. Wang, R.; Li, D.; Miao, K. Optimized radial basis function neural network based intelligent control algorithm of unmanned surface vehicles. *J. Mar. Sci. Eng.* **2020**, *8*, 210. [CrossRef]
23. Wang, Z.; Qiu, C.; Dong, Z.; Cheng, S.; Zheng, L.; Chen, S. Trajectory tracking of unmanned surface vessels based on robust neural networks and adaptive control. *J. Mar. Sci. Eng.* **2025**, *13*, 1341. [CrossRef]
24. Dong, S.; Wu, C.; Wang, B.; Wu, Z.-G.; Liu, M. Data-driven fault-tolerant path-following control for USV based on fixed-time guidance and fuzzy disturbance observer. *Nonlinear Dyn.* **2025**, *113*, 29613–29632. [CrossRef]
25. Chen, G.; Wang, W.; Dong, J. Performance-optimize adaptive robust tracking control for USV-UAV heterogeneous systems with uncertainty. *IEEE Trans. Veh. Technol.* **2025**, *74*, 7251–7262. [CrossRef]
26. Zhao, C.; Yan, H.; Gao, D.; Wang, R.; Li, Q. Adaptive neural network iterative sliding mode course tracking control for unmanned surface vessels. *J. Math.* **2022**, *2022*, 1417704. [CrossRef]
27. Zhang, H.G.; Zhang, X.K.; Bu, R.X. Radial basis function neural network sliding mode control for ship path following based on position prediction. *J. Mar. Sci. Eng.* **2021**, *9*, 1055. [CrossRef]
28. Wang, W.; Wang, T.; Zhang, D.; Zhang, G.; Wang, N.; Hao, Z. Adaptive course keeping control for rudder angle constraint nonlinear ship systems with dead-zone input and uncertain control coefficients. *Ocean Eng.* **2025**, *342*, 122994. [CrossRef]
29. Xie, M.; Wu, Z.; Huang, H. Low-complexity formation control of marine vehicle system based on prescribed performance. *Nonlinear Dyn.* **2024**, *112*, 18311–18332. [CrossRef]
30. Gonzalez-Garcia, A.; Castañeda, H. Adaptive integral terminal sliding mode control for an unmanned surface vehicle against external disturbances. *IFAC-Pap. OnLine* **2021**, *54*, 202–207. [CrossRef]
31. Gonzalez-Garcia, A.; Castañeda, H. Guidance and control based on adaptive sliding mode strategy for a USV subject to uncertainties. *IEEE J. Ocean. Eng.* **2021**, *46*, 1144–1154. [CrossRef]
32. Zhao, K.; Song, Y.; Chen, C.L.P.; Chen, L. Adaptive asymptotic tracking with global performance for nonlinear systems with unknown control directions. *IEEE Trans. Autom. Control* **2021**, *67*, 1566–1573. [CrossRef]

33. Ye, X.; Jiang, J. Adaptive nonlinear design without a priori knowledge of control directions. *IEEE Trans. Autom. Control* **1998**, *43*, 1617–1621. [CrossRef]
34. Lin, B.; Xie, W.; Shi, Y.; Du, B.; Zhang, C.; Zhang, W. Robust target interception strategy for a USV with experimental validation. *IEEE Robot. Autom. Lett.* **2023**, *8*, 7042–7049. [CrossRef]
35. Islam, M.M.; Siffat, S.A.; Ahmad, I.; Liaquat, M. Supertwisting and terminal sliding mode control of course keeping for ships by using particle swarm optimization. *Ocean Eng.* **2022**, *266*, 112942. [CrossRef]
36. Wang, Q.; Sun, C.; Chen, Y. Adaptive neural network control for course-keeping of ships with input constraints. *Trans. Inst. Meas. Control* **2019**, *41*, 1010–1018. [CrossRef]
37. Wu, G.X.; Ding, Y.; Tezdogan, T.; Incecik, A. Adaptive neural network and extended state observer-based non-singular terminal sliding mode tracking control for an underactuated USV with unknown uncertainties. *Appl. Ocean Res.* **2023**, *135*, 103560. [CrossRef]
38. Ye, H.; Wu, S.; Liu, W.; Yang, X.; Du, Z.; Xue, W. Adaptive neural synergetic heading control for USVs with unknown dynamics and disturbances. *Ocean Eng.* **2024**, *300*, 117438. [CrossRef]

Disclaimer/Publisher's Note: The statements, opinions and data contained in all publications are solely those of the individual author(s) and contributor(s) and not of MDPI and/or the editor(s). MDPI and/or the editor(s) disclaim responsibility for any injury to people or property resulting from any ideas, methods, instructions or products referred to in the content.